

The Effect of Effusion Holes Inclination Angle on the Adiabatic Film Cooling Effectiveness in a Three-Sector Gas Turbine Combustor Rig with a Realistic Swirling Flow

Antonio Andreini^{a,*}, Riccardo Becchi^a, Bruno Facchini^a, Alessio Picchi^a, Antonio Peschiulli^b

^a*Department of Industrial Engineering DIEF, University of Florence, Via di Santa Marta 3, 50139 Florence, Italy*

^b*GE Avio S.R.L. - Via I Maggio, 99, 10040, Rivalta di Torino (TO), Italy*

Abstract

The introduction of Lean Burn concept as basic Low- NO_x scheme for future aero-engines is heavily affecting the aero-thermal design of combustors. A great amount of air is admitted through the injection system with relevant swirl components, producing very complex flow structures (recirculations, vortex breakdown) for flame stabilization. As a consequence a reduced quantity of air is available for liner cooling, pushing the adoption of high effectiveness cooling schemes. Effusion cooling represents one of the first choices due to its low weight and a relatively easy manufacturability. Liner metal temperature is kept low by the combined protective effect of coolant film, heat removal inside holes and an improved cold-side convection. In lean burn systems the evolution of film protection can be heavily influenced by the swirl flow interaction with combustor walls.

The subject of this work is to investigate the effects of the realistic flow field of a lean burn injector on the adiabatic film cooling effectiveness on an effusion cooled combustor liner. A dedicated three-sector rig was designed with the aim of measuring film effectiveness with Pressure Sensitive Paint technique. Three effusion cooling geometries with different inclination angles were tested at various levels of pressure drops across the perforation, resulting in different blowing ratio values. It was also taken into consideration several flow rate levels of starter film realized by spent dome cooling air, injected through a dedicated plain slot. The analysis of film effectiveness measurements were supported by flow field investigation in the near wall region carried out by means of Particle Image Velocimetry.

Results pointed out the relevant impact of combustor flow field on the adiabatic film cooling effectiveness as well as a significant role of the inclination angle, recommending a careful revision of standard design practices based on one dimensional flow assumption and suggesting possible holes arrangement optimization.

Keywords: Gas Turbine, Combustor, Liner, Effusion cooling, Adiabatic Film Cooling Effectiveness, Swirl flows, PSP, PIV

*Corresponding Author

Email address: antonio.andreini@unifi.it (Antonio Andreini)

Nomenclature

Acronyms

<i>BR</i>	Blowing Ratio [-]
<i>CCD</i>	Charged Coupled Device
<i>Cd</i>	Discharge coefficient [-]
<i>CR</i>	Corner Recirculation
<i>DR</i>	Density Ratio [-]
<i>IR</i>	Inner Recirculation
<i>NO_x</i>	Nitrogen Oxides
<i>PERM</i>	Partial Evaporation and Rapid Mixing
<i>PIV</i>	Particle Image Velocimetry
<i>PMMA</i>	Poly-Methyl Methacrylate
<i>PSP</i>	Pressure Sensitive Paint
<i>Re</i>	Reynolds number [-]
<i>S_N</i>	Swirl Number [-]

Greek symbols

α	Injection angle [<i>deg</i>]
η	Film Cooling Effectiveness
σ	Perforation porosity [-]
θ	Tangential direction in swirler flow [-]

Latin symbols

\dot{m}	Mass flow [<i>g/s</i>]
<i>A</i>	Area [<i>m</i> ²]
<i>C</i>	Mass fraction [-]
<i>D</i>	Diameter [<i>m</i>]
<i>d</i>	Holes diameter [<i>m</i>]

<i>G</i>	Momentum flux [<i>kg/m/s</i> ²]
<i>P</i>	Static pressure [<i>Pa</i>]
<i>S</i>	Hole pitch [<i>m</i>]
<i>T</i>	Temperature [<i>K</i>]
<i>V</i>	Velocity [<i>m/s</i>]
<i>W</i>	Slot coolant consumption [-]
<i>x</i>	Stream-wise, axial direction [<i>m</i>]
<i>y</i>	Span-wise, lateral direction [<i>m</i>]
<i>z</i>	Orthogonal to test plate direction [<i>m</i>]

Subscripts

<i>ad</i>	adiabatic
<i>aw</i>	adiabatic wall
<i>cool</i>	cooling flow
<i>eff</i>	effusion flow
<i>h</i>	hydraulic
<i>in</i>	inlet
<i>main</i>	mainstream
<i>max</i>	maximum
<i>out</i>	outlet
<i>slot</i>	slot cooling system
<i>sw</i>	swirler
<i>w</i>	wall
<i>x</i>	axial direction
<i>y</i>	lateral direction
<i>z</i>	orthogonal to test plate direction

1. Introduction

In modern gas turbine combustors the process of flame stabilization and anchoring is widely based on the use of swirling flows. Combustion air is delivered as swirling jets in single or multiple configurations. The objective is to promote the so-called vortex breakdown process, which is the base flow structure of swirl stabilized flames. With this type of flow, wide low speed regions are produced by the onset of inner and outer recirculations, supporting local flame anchoring. Recirculating flows allow to have a continuous supply of high temperature gases to incoming fresh mixture, while the strong velocity gradients and flow unsteadiness greatly enhance free stream turbulence which improves the overall reaction and mixing rates. This type of flame stabilization process has become more and more common and exasperated with the widespread use of lean flames for reduction of NO_x emissions, firstly adopted in heavy duty gas turbines [1], and more recently considered also for aero-engine combustors to fulfil the future emissions standards [2].

A common characteristics of lean burn gas turbine combustors is the great amount of air delivered by the fuel-air injection system, that can reach 70 – 75% of total combustor air. This means a strong reduction of air available for liner wall cooling, forcing to the introduction of high effectiveness cooling schemes. Among different possible solutions, effusion cooling (or full coverage film cooling) certainly represents one of the most promising technology. It is based on the injection of cooling air through a dense pattern of small diameter holes drilled on the liner. The purpose is to generate an high effectiveness layer of coolant on the liner surface, avoiding its direct exposure to hot gases, and to provide heat removal by forced convection inside each hole. An additional positive contribution to overall cooling effectiveness may come to an increased convective heat transfer on the cold-side of the liner due to the suction effect of coolant flow near the rim of each effusion holes. Thanks to the relative simple manufacturing process involved and a reduced impact on combustor weight, effusion is one the first options, especially in aero-engine applications. A recent review on effusion cooling concept with a discussion about the basics related to hole spacing and coolant-hot-gas interaction can be found in Krewinkel [3], where some perspectives about the application of effusion cooling to turbine blade cooling are also reported. More specific assessments regarding the application of effusion cooling to combustor liner with fundamental analysis about the relative weight of the three main contributions to overall cooling effectiveness can be found in Martiny et al. [4] and more recently in Gerendás et al. [5] and Andreini et al. [6].

The engineering problem of applying effusion to combustor liner cooling, together with all related physical aspects, has been widely analysed over the last 40 years, with several contributions available in the open literature. In particular most part of the studies have usually been aimed at investigating the role of the various flow and geometric parameters on the film cooling effectiveness, generally with simplified configurations (flat plates with uniform mainstream flow). One of the first contribution is due to Kasagi et al. [7] where the overall cooling effectiveness of full coverage film cooling plates was measured at different blowing ratios with liquid crystals technique. The focus was put on the the role of thermal properties of the plate material. Among the pioneering studies it is worth to cite the contributions by Andrews and co-workers [8, 9, 10] where

37 the effects on film effectiveness of several parameters, as the number of holes, length and arrangement, were
38 investigated. In their study, Martiny et al. [11] evaluated row by row adiabatic film effectiveness (via Infra-
39 Red thermography) and performed flow visualizations (by means of Schlieren photography) on a full coverage
40 film cooling plate with highly inclined holes (17°) at different blowing ratios (0.5 to 4.0). It was observed
41 that, even with high blowing ratio and therefore with full penetration of jets, an appreciable cooling benefit
42 can be measured in terms of adiabatic film effectiveness. This is due to a reduction of gas temperature in the
43 mixing region contributing to keep near wall temperature low even without the presence of a coherent film:
44 this is expected to be the process in actual combustor where high blowing ratios are commonly observed.

45 An extensive parametric study was later realized by Gustafsson and Johansson [12] where overall cool-
46 ing effectiveness was tested with Infra-Red thermography. A large database was obtained varying several
47 flow and geometric parameters, nevertheless results in terms of overall cooling effectiveness do not permit
48 to accurately separate the effects on adiabatic film effectiveness and heat transfer. In the contribution by
49 Harrington et al. [13] the effect of an increasing free stream turbulence on the adiabatic film effectiveness was
50 analysed for normal injection holes. A reduction of film coverage is observed when turbulence increases, but
51 the impact is largely reduced with blowing ratios approaching 1.0. More recently Martin and Thorpe [14]
52 observed an increase of adiabatic effectiveness with realistic high free stream turbulence when using inclined
53 holes at blowing ratio above 1.0: this is due to an increased mixing rate of the jet with the mainstream, which
54 enhance the amount of coolant close to wall region. The investigation carried out by Scrittore et al. [15] was
55 focused on the measurement of adiabatic film effectiveness and flow field from inclined effusion cooling jets in
56 a range of blowing ratios (3.2 to 5.0) that can be observed in actual combustors. A large number of effusion
57 rows was considered (20) permitting to observe the achievement of fully developed film after the 15th row.
58 In their recent study, Ligrani et al. [16] showed adiabatic film effectiveness and heat transfer for full coverage
59 film cooling configurations in the presence of a streamwise pressure gradient; the effect of the blowing ratio
60 and the influence of dense/sparse hole arrays on the thermal effectiveness are discussed.

61 One of the most important parameter affecting the final adiabatic film effectiveness of multi row effusion
62 cooling is certainly the inclination angle of the holes. Among the first systematic studies concerning this
63 aspect is worth to be mentioned Foster and Lampard [17] who analysed the effects of the injection angle in-
64 vestigating a set of geometries with $\alpha = 35^\circ, 55^\circ, 90^\circ$. Great dependence from this parameter was observed,
65 with small injection angle that showed the highest cooling effectiveness at low blowing ratios, while large
66 injection angles were advantageous at high blowing ratios. Coming to more recent contributions, Hale et al.
67 [18] performed a parametric study for a single row of short holes, fed by a narrow plenum, with two different
68 injection angles (35° and 90°). Results highlighted that under specific conditions, similar or improved cover-
69 age was achieved with orthogonal injection compared with 35° holes. An investigation carried out by Baldauf
70 et al. [19] indicated optimum flow conditions for efficient cooling for a wide range of configurations, among
71 which it's worth to mention three different streamwise angle levels ($30^\circ, 60^\circ, 90^\circ$). The same range of angles
72 were investigated by Yuen and Martinez-Botas [20] in a flat plate test facility with a zero pressure gradient

73 for a wide range of blowing ratios. Behrendt et al. [21] presented results about the characterization of the
74 film effectiveness of advanced combustor cooling concepts at realistic operating conditions. They observed
75 an effectiveness improvement at lower cooling hole angles (20°) due to the reduced penetration depth of the
76 cooling air jets. More recently Andreini et al. [22] carried out an investigation on several multi-perforated
77 plates measuring the adiabatic film effectiveness by using Pressure Sensitive Paint technique on a flat plate
78 test rig. A comparison between 30° and 90° at different blowing ratios was discussed, pointing out the role
79 of different free-stream turbulence levels and coolant to mainstream density ratio.

80 All the above mentioned works regarding effusion cooling are based on simple mainstream flow fields
81 (i.e., uniform velocity). First attempts to take into account actual combustor flow field features are due for
82 instance to Scrittore et al. [23] and later to Ceccherini et al. [24], where the interactions of effusion cooling
83 flow with dilution jets or starter film cooling were investigated on single flat plate configurations. The use
84 of high swirling flows for flame stabilization purposes may result in a great interaction between swirl jet and
85 combustor liner, which can deeply affect both convective heat transfer and film cooling protection. Very few
86 studies can be found in the open literature where the investigation of such effects are reported. It's worth
87 to be recalled the pioneering studies realized at the Karlsruhe Institute of Technology (KIT) [25, 26], where
88 effusion cooling effectiveness in a three sector rig with realistic lean direct injection nozzles was measured
89 by Infra-Red thermography. More recently, Andreini and co-workers [27, 28] carried out an experimental
90 survey aimed at measuring adiabatic film cooling effectiveness and heat transfer coefficient in a planar three
91 sector rig operated with a representative swirling flow field: a cooling scheme based on effusion with slot
92 cooling was considered. In both studies, a specific configuration of multi-perforated liner was used, without a
93 systematic deepening about the role of geometric parameters on cooling effectiveness. A similar investigation
94 was recently carried out by Ge et al. [29] with Infra-Red thermography in reactive conditions but with a
95 reduced number of effusion rows: the authors point out a complex measurement process in presence of the
96 heat release due to combustion which affects the accuracy of the obtained results.

97 The aim of the present study is to deepen the knowledge on film cooling interaction with highly swirling
98 flows in realistic combustor flow field environment, exploring the impact on adiabatic film cooling effective-
99 ness when varying one of the most critical parameter: the coolant injection angle.

100

101 **2. Experimental setup**

102 *2.1. Experimental geometry*

103 Experiments were carried out in an open loop wind tunnel device reported installed at the THT-Lab of
104 the University of Florence, Italy: schematic representation is reported in Figure 1. The test rig was devel-
105 oped within the European Research project LEMCOTEC (Low Emissions Core-Engine Technologies) [30]
106 and consists of a planar three-sector combustor operating at ambient conditions without reactive processes.
107 It is equipped with a complete cooling scheme composed of a slot system and multi-perforated liners whose

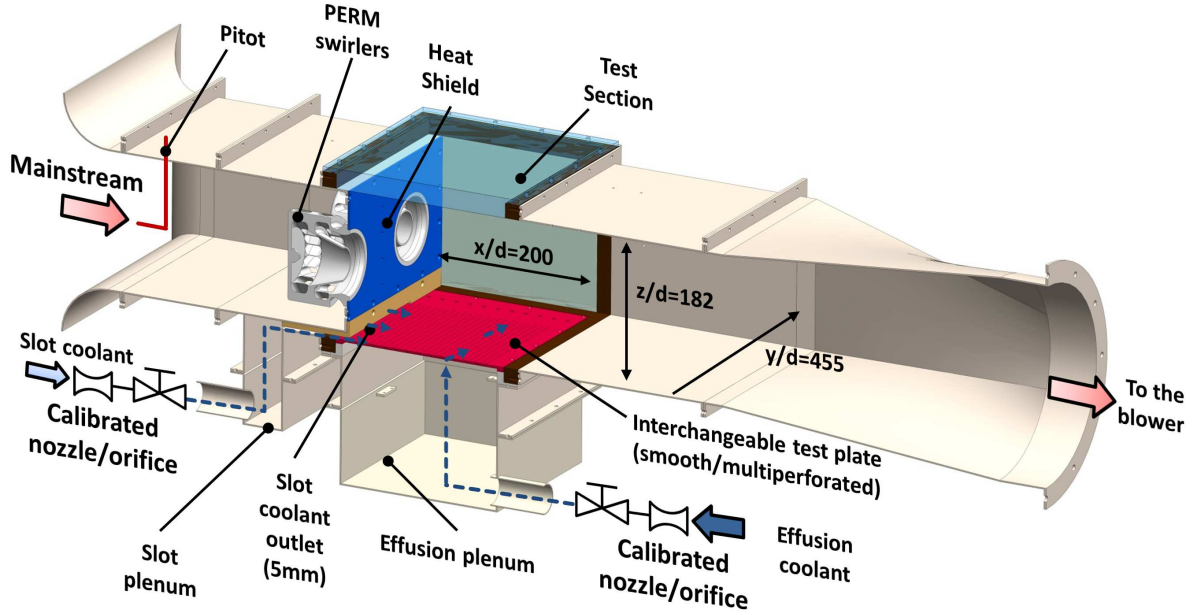


Figure 1: Cross sectional view of the test rig

108 mass flow rates can be controlled independently. The mainstream flow is delivered by three injectors which
 109 produce a flow field representative of a swirl stabilized combustor. Details of the swirler geometry will be
 110 discussed in a following section.

111 The experimental tests were designed to work at ambient pressure and near ambient temperature con-
 112 ditions, so allowing the use of Pressure Sensitive Paint (organic compound). An enlarged scale factor was
 113 selected with respect to reference engine in order to replicate Reynolds number and pressure drop of the
 114 swirlers with respect to the engine nominal conditions.

115 The mainstream flow is fed inside the test rig by means of a 90 kW centrifugal blower and enters inside
 116 the test section, which reproduces an aero-engine lean combustor, after being swirled by the injectors. The
 117 inner liner of the chamber is represented by a multi-perforated plate and is fed by an upstream large plenum

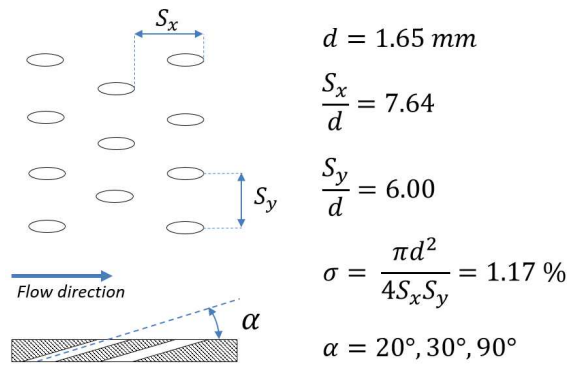


Figure 2: Summary of effusion perforation geometry

118 chamber. During the experimental campaign three different effusion liner geometries were investigated vary-
119 ing the holes injection angle (evaluated with respect to liner surface along nominal mainstream direction):
120 tested angles are 20° , 30° and 90° . All the effusion plates share the same holes pattern: 1184 cylindrical
121 holes are arranged in a staggered array counting for a total of 23 rows, with the first row located about
122 $0.22S_x$ from the beginning of the liner. Scaled holes diameter is equal to $d = 1.65 \text{ mm}$ in all cases, while
123 normalized streamwise and spanwise pitches are respectively $S_x/d = 7.64$ and $S_y/d = 6$. This common
124 diameter and holes arrangement leads to a common plate porosity of about 1.17%: porosity is here defined
125 as the ratio between holes aperture and overall plate surface. A summary of the principal geometric data of
126 multiperforations is shown in Figure 2.

127 The slot exit is positioned on the dome wall below the three injectors. It has a constant height of 5mm and a
128 width equal to 2 times the swirlers pitch. For both the cooling systems, air passes through screens and flow
129 straighteners upstream of the injection, and the mass flow rates are set by adjusting two manual ball valves.

130 The test section has a length in the flow direction equal to $x/d = 200$, a width of $y/d = 455$ and an height
131 of $z/d = 182$. The lateral walls and the top side of the chamber, located in opposite position with respect
132 to the multi-perforated liner, are made in a transparent material (in this case Poly-Methyl MethAcrylate
133 (PMMA)) in order to allow wide optical accesses for both adiabatic film cooling effectiveness tests and PIV
134 measurements. Downstream of the test section, the mainstream and the mixed cooling flows pass through a
135 constant cross-section channel and a smooth converging duct before flowing towards the silencer installed at
136 the blower inlet.

137 The pressure drop across the swirlers and consequently the mainstream mass flow rate is imposed acting
138 on the rotating speed of the centrifugal blower by means of an inverter. The mass flow rate is measured by
139 means of a Pitot tube, located downstream of the rig inlet bell mouth, and double checked evaluating the
140 injectors pressure drop, assumed as known the effective passage area. The uncertainty of the main mass flow
141 measurement is $\pm 6\%$ with a level of confidence of 95%. Calibrated nozzles, installed in two dedicated feeding
142 ducts positioned upstream of the coolant plena, are used to evaluate the slot and effusion mass flow rates
143 with an uncertainty of $\pm 5\%$. T type thermocouples (uncertainty $\pm 0.5 \text{ K}$ with level of confidence of 95%) are
144 employed to monitor the flow temperature in several locations of the rig with the data acquisition provided
145 by an HP/Agilent[®] 34972A unit. A pressure scanner Scanivalve[®] DSA 3217 with temperature compensated
146 piezoresistive relative pressure sensors measures the static pressure in 13 different locations with a maximum
147 uncertainty of $\pm 7 \text{ Pa}$ (level of confidence of approximately 95%).

148

149 2.2. Swirler geometry

150 The apparatus is characterized by the presence of three air spray swirlers designed by GE-Avio. The
151 objective of the design is to realize a device capable of Ultra Low NO_x operations through a lean, swirl
152 stabilized, spray flame [31]. The injectors, called PERM (Partial Evaporation and Rapid Mixing), are
153 characterized by two radial co-rotating swirlers which have the role of producing a highly swirling flow at the

154 outlet section of the nozzle (Figure 3). The final outcome is the achievement of a large inner recirculation
 155 region surrounded by an high velocity annular jet, which represents the main flow structures of typical swirl
 156 stabilized flames.

According to the review of Lilley [32], the onset of the vortex breakdown process, and the related presence

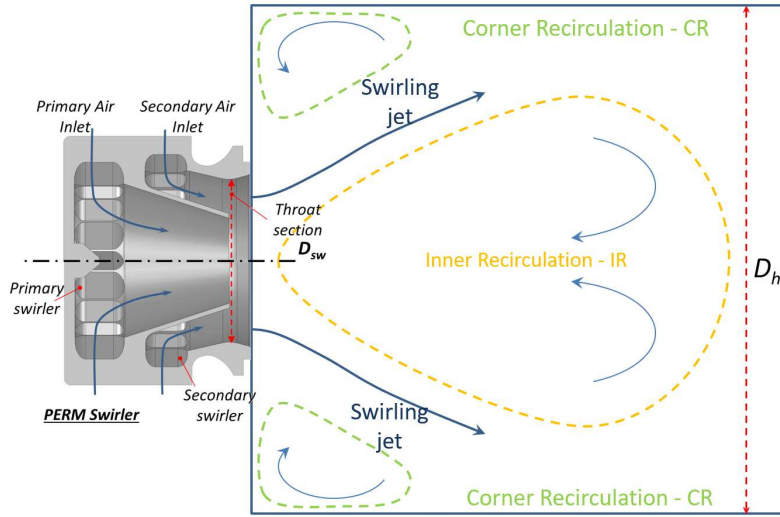


Figure 3: Geometry of the adopted swirler injectors

157 of a central toroidal recirculation region, can be established by a proper sizing of the swirling intensity of
 158 the flow. The common criteria is to introduce the so-called Swirl Number (S_N) which is defined as the ratio
 159 between the axial flux of circumferential momentum G_θ and the axial momentum flux G_x :
 160

$$S_N = \frac{G_\theta}{R_0 G_x} \quad (1)$$

161 where R_0 represents a characteristic dimension of the swirler. A Swirl Number greater than 0.5-0.6 may result
 162 in strong not equilibrated radial and axial pressure gradients which induce main vortex collapse (breakdown).

163 As discussed in Marinov et al. [31], a swirl number of 0.75 is prescribed at the throat section of the in-
 164 vestigated nozzles ($R_0 = 0.5D_{sw}$), with a highly uniform velocity distribution along the tangential direction.
 165 A fundamental geometric parameter affecting the stability of the flame by acting on the size of the central
 166 recirculation region, is the expansion ratio (see for instance Fu et al. [33] or Andrews et al. [34]) defined as the
 167 ratio between combustion chamber hydraulic diameter and nozzle diameter (D_h/D_{sw} according to Figure 3):
 168 a value of 2.5 can be observed in the case of PERM design. All the features of the PERM injector discussed
 169 above allow to generate a flow field that can be considered representative of a typical lean direct injection
 170 burning system for modern aero-engine combustors.

171

172 2.3. PSP technique

173 In order to estimate the film covering performance of the three effusion geometries and to evaluate the
 174 mutual effects between coolant and the mainstream swirled flow, a Pressure Sensitive Paint technique was

175 employed in the central region of the liner.

176 Thanks to the luminescence behaviour due to their chemical composition, PSP can be exploited as a re-
177 liable detector of fluid oxygen concentration close to the paint layer and hence used for film effectiveness
178 measurements based on heat and mass transfer analogy (gas concentration technique). Since the governing
179 equations for heat and mass transfer phenomena are similar, the solutions of the two analogous problems
180 are identical if the boundary conditions are the same and if the molecular/turbulent Schmidt number are
181 identical to molecular/turbulent Prandtl number (i.e. Lewis number equal to one). As reported by several
182 authors, turbulent flow are characterized by a turbulent Lewis number roughly equal to one as required
183 by the analogy [35]. Regarding the applicability of the heat and mass transfer analogy in the investigated
184 case - effusion cooling with highly swirled turbulent flow and cooling jets in penetration regime - the mixing
185 process is mainly located far from the test plate where the turbulence effects are dominant, and hence the
186 analogy can be considered satisfied. It is worth notice that, even if the hypothesis of unity turbulent Lewis is
187 usually met, the similarity of molecular diffusion may not be satisfied. In the present test case the molecular
188 quantities influence the heat and mass transfer phenomena in the viscous sub layer near the wall. However, a
189 lower influence of molecular parameter in this region is expected due to the zero concentration/temperature
190 gradient at the adiabatic/non-permeable liner wall.

191 Therefore, assuming valid the heat and mass transfer analogy and using a tracer gas without free oxy-
192 gen as coolant, is possible to estimate the adiabatic film cooling effectiveness distribution on the liner [36]
193 according to the following equations:

$$\eta_{ad} = \frac{T_{main} - T_{aw}}{T_{main} - T_{cool}} \equiv \frac{C_{main} - C_w}{C_{main}} \quad (2)$$

194 where C_{main} and C_w are oxygen concentration respectively in the main free stream and in proximity of the
195 wall.

196 For further information, an extensive description of the technique operating principles and the experi-
197 mental procedure are reported in previous works conducted by the authors [37][28].

As shown in Figure 4, the central region of the liner geometry was sprayed with several light coats of

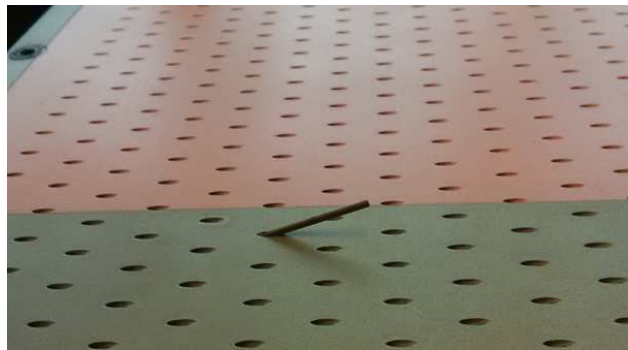


Figure 4: 20° effusion plate covered with PSP

198

199 PSP. The paint employed was provided by Innovative Scientific Solutions Inc., and it was composed by a

200 blend of Fluoro Isopropyl Butyl polymer (FIB) and Platinum tetra(pentafluorophenyl) porphyrin (PtTFPP).
 201 During realized tests the paint was excited with an high performance led illuminator DLR-IL104[®] and the
 202 emission was captured by a 1600x1200 resolution 14-bit CCD camera PCO.1600. The selected foreign gas
 203 used to perform adiabatic film cooling effectiveness tests is nitrogen. Two dedicated feeding lines, equipped
 204 with calibrated orifices, are employed to feed the effusion and the slot plenum chamber, from a 10bar pressure
 205 tank where the N_2 is stored.

206 The uncertainty of adiabatic film cooling effectiveness measurements was evaluated following the method
 207 proposed by Kline and McClintock [38], achieving values around 10% for $\eta_{ad} = 0.2$ and 3% for regions where
 208 $\eta_{ad} > 0.8$.

209
 210 *2.4. PIV measurements*

211 Particle Image Velocimetry campaign was aimed at supporting the adiabatic film cooling effectiveness
 212 measurements in order to deeply understand the complex interactions between main swirled flow and the
 213 cooling flows. For this purpose three investigation planes were selected: the first, *Center* plane, is the merid-
 214 ian projection perpendicular to the liner test plate and passing trough the center of the central swirler, while
 215 the second, *Median* plane, is parallel to combustor liner passing through the axis of the injector and finally
 216 the third is the *Wall* plane located 5mm above the liner (Figure 5). With the effusion cooling flow enabled,
 217 PIV measurements were realized on center plane only, focusing the attention on the corner region underneath
 218 the central injector. The laser sheet (1mm thickness) was introduced through the top side PMMA window
 219 involving the use of a 45° inclined mirror, while the optical access for the camera was obtained from one of
 220 the transparent lateral walls. As a tracer, 1 μ m diameter olive oil particles were used, employing a Laskin
 221 nozzle for their generation. The injection takes place, through a perforated pipe, immediately downstream
 222 of the rig inlet bell mouth, alongside its whole height.

223 Two different camera/laser positions were necessary to cover, with enough image resolution, the estab-

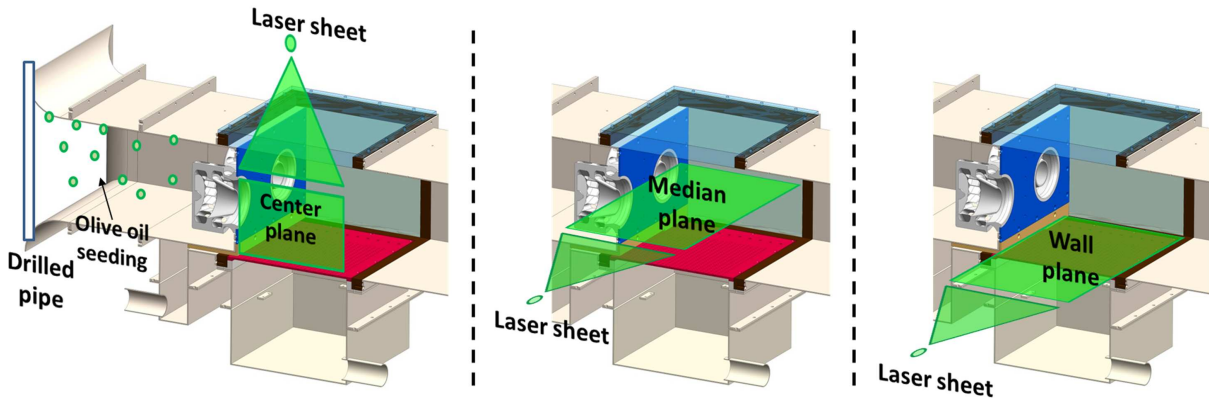


Figure 5: Position of the PIV measurement planes

224 lished investigation area, including a $5mm$ overlap to avoid loss of information in the neighbouring regions. A
 225 large number of image pairs were acquired, setting a time delay between the two laser pulses of about $10\mu s$,
 226 finally an iterative procedure based on an adaptive cross-correlation method was performed to obtain the
 227 velocity field distributions. Measurements were carried out using a Dantec Dynamics PIV system, based on a
 228 $120mJ$ New Wave Solo Nd:YAG pulsed laser (wavelength of $532nm$). For the effusion geometry with 30° holes
 229 inclination angle, a FlowSense $2Mpixel$ camera operating at a data rate of $15Hz$ was employed, with control
 230 and post-processing operations managed by means of the commercial software Dantec FlowManager[®]. For
 231 the other two multi-perforated plates was involved a SpeedSense $4Mpixel$ camera, coupled with the Dantec
 232 Dynamic Studio[®]. software.

233 Employing the method proposed by Westerweel [39] and considering a particle displacements varying from
 234 5 to 10 pixels, measurements uncertainty in the mean velocity is estimated around 3%.

235 2.5. Test conditions

236 PSP measurements were conducted for all the three effusion geometries characterized by different injection
 237 angle, while PIV investigation wasn't performed for the 20° configuration because not significant variations
 238 were expected with respect to the already tested 30° . The whole experimental campaign was performed
 239 imposing representative operating flow conditions both for the mainstream and the cooling lines and repli-
 240 cating the relevant non dimensional parameters. The pressure drop across the set of swirlers was evaluated
 241 by means of multiple static pressure taps located upstream the dome (P_{in}) and downstream the investigated
 242 liner region near the outlet section (P_{out}). The pressure drop was maintained constant at the reference value
 243 of 3.5%:

$$\frac{\Delta P}{P} = \frac{P_{in} - P_{out}}{P_{in}} \quad (3)$$

244 With the imposed pressure drop, values of mainstream Reynolds number of about 160000 were achieved,
 245 considering the hydraulic diameter of the test section ($D_h/d = 260$) as the reference length. Regarding
 246 the cooling line, first focussing on the effusion system, the coolant was set acting on the pressure drop across
 247 the plate:

$$\Delta P/P_{eff} = \frac{P_{eff} - P_{out}}{P_{eff}} \quad (4)$$

248 where P_{eff} represent the static pressure measured inside the feeding plenum. Different different mass flow
 249 rates were tested, with the reference effusion pressure drop set at 3%. **The pressure drop across the perforation**
 250 **was selected as the controlling parameter of coolant flow according to the operations of the real engine.**
 251 Regarding the slot system, the test conditions are imposed through the coolant consumption parameter W ,
 252 defined as the ratio between slot and mainstream mass flow rate related to the central swirler.

$$W = \frac{\dot{m}_{slot}}{\dot{m}_{main}} \cdot \frac{3}{2} \quad (5)$$

253 Tests were carried out for two levels of coolant consumption: with slot system disabled and with the actual
 254 combustor flow split $W = 3\%$. Highest Reynolds number of effusion jets, obtained with the maximum

Main flow	Effusion flow	Slot flow
<i>Air</i>	$N_2 - Air(PIV)$	$N_2 - Air(PIV)$
$T_{main} = 300K$	$T_{eff} = 300K$	$T_{slot} = 300K$
$Re_{main} = 160000$	$Re_{eff} = 0 - 4000$	$Re_{slot} = 0 - 3500$
$\Delta P/P = 3.5\%$	$\Delta P/P_{eff} = 0 - 1 - 2 - 3\%$	$W = 0 - 3\%$

Table 1: Test matrix

255 pressure drop, is 4000, while for the slot mass flow the greatest Reynolds, based on slot height, is 3500.

256 For the whole experimental campaign, mainstream flow is air at ambient conditions, regarding the coolant
257 flows, air is employed for PIV test while Nitrogen was used to perform PSP measurements resulting in a
258 coolant to mainstream density ratio equal to 1.

259 During the commissioning phase of the test rig, the three test plates where separately flow checked
260 imposing the same conditions in terms of tested pressure drop in order to asses the values of discharge
261 coefficients (Cd). The two test plates with slant injection angle highlighted a Cd approximately equal to
262 0.67, while the normal hole perforation exhibited an higher discharge coefficient close to 0.75 as already
263 documented by Others in the open literature [40].

264 Each geometry was tested at the same pressure drop levels. According to the different effective areas
265 of the perforations, the 20° and 30° plates have a ratio between effusion and mainstream mass flow on the
266 central sector in the range $7.5 - 13\%$ when varying the $\Delta P/P_{eff}$, on the other hand the coolant consumption
267 for the plate with normal holes is in the range $8.4 - 14.5\%$. All the test conditions are summarized in Table 1.

268 The main issue related to the adopted test conditions is the reduced level of density ratio with respect to
269 expected actual engine condition ($DR \approx 2.5$). The density ratio has an impact on the adiabatic film cooling
270 effectiveness distribution particularly in the transition between mass addition and penetration regime and
271 its effect seems to be negligible in full penetration regime [41]. These aspects have been already debated by
272 the Authors by means of a dedicated experimental survey using effusion plates with uniform flow conditions
273 [22]. However, considering the expected effusion flow field, mainly in penetration regime, and the pure
274 comparative purpose of the survey, the main outcomes of the work can be considered unaffected by the lack
275 of DR similitude.

276 3. Results

277 3.1. Flow field investigation - Case without effusion cooling

278 Before analyzing the behaviour of the effusion cooling process, a description of the flow field generated
279 by the adopted swirlers will be reported. According to its high swirl number and expansion factor, the
280 swirling jet delivered by the nozzles quickly breakdown when entering in the chamber, with the generation
281 of a large inner recirculation region. As a consequence of the abrupt change in cross section, the swirling jets
282 trigger two recirculating regions in the outer corners between liners and heat shield. An high speed annular

283 swirling jet is observed between central and corner recirculations. Such flow structures are clearly shown
 284 in Figure 6 where flow field measured by the described PIV technique is reported on the previously defined
 285 Center plane: the value U_{max} used to normalize the velocity is, for all the shown maps, 50 m/s. The near
 286 wall region up to effusion row 14 is interested by a very complex flow field which is expected to heavily affect
 287 the development of the film. In particular it can be observed a reverse flow up to the 5th row, due to corner
 288 recirculation, followed by a stagnation area where the swirling jet collides with the liner (between rows 5 and
 289 8). Downstream of the 8th row a strong flow acceleration can be observed, while after row 14 the flow begins
 290 to develop in a smoother way. As it will clearly results from the discussion of adiabatic film effectiveness
 291 measurements, a significant impact on effusion cooling jets mixing is observed in this region.

292 To better understand the swirler flow field, the results obtained on an additional PIV frame are shown
 293 in Figure 7 which shows the streamlines on the median plane. Thanks to this visualization the complete

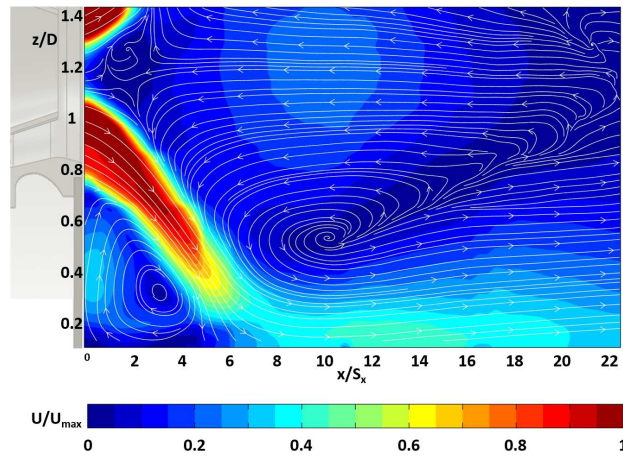


Figure 6: Flow field with no coolant injection on the central meridian plane

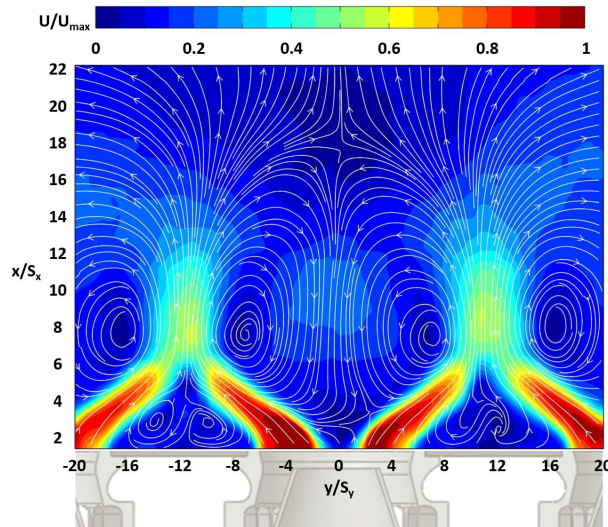


Figure 7: Flow field with no coolant injection on the median plane

294 extension of the central recirculation regions can be clearly pointed out. It is also important to observe the
 295 almost exact symmetry of the inner recirculation generated by the central nozzle respect to swirler axis. This
 296 finding confirms the proper design of the rig with representative results coming from investigations on the
 297 central sector.

298 Contour plot depicted in Figure 8 highlights the main flow direction close to liner surface: reverse flow is
 299 observed upstream of the stagnation region, while more downstream the flow is gradually losing the residual
 300 swirling component. This velocity map will be used in the following to provide an estimation of effusion jets
 301 Blowing Ratio.

302 Exploiting available CFD results obtained on the present geometry with an Hybrid RANS/LES approach,
 303 which proved to perfectly match the measured flow field (see Mazzei et al. [42] for additional details), more
 304 quantitative evaluations of the flow field were carried out. First of all the swirl number in the throat section
 305 of the central nozzle was verified. According to the definition provided in previous sections, the computed
 306 swirl number is 0.77 which is fairly close to the nominal expected design value of 0.75. Mass flow rates
 307 entering into the inner region, \dot{m}_{IR} , and into the corner region, \dot{m}_{CR} , are computed to be respectively 57%
 308 and 38% of the mass flow delivered by the swirler.

309

310 3.2. Flow field investigation - Effect of effusion cooling

311 Results of Figure 9 highlight deep modifications in the flow field varying the coolant injection angle and
 312 strong interaction phenomena near the wall between the mainstream and the cooling flows. A different ex-
 313 tension of the investigation area was achieved for the two configurations, both covering however the region

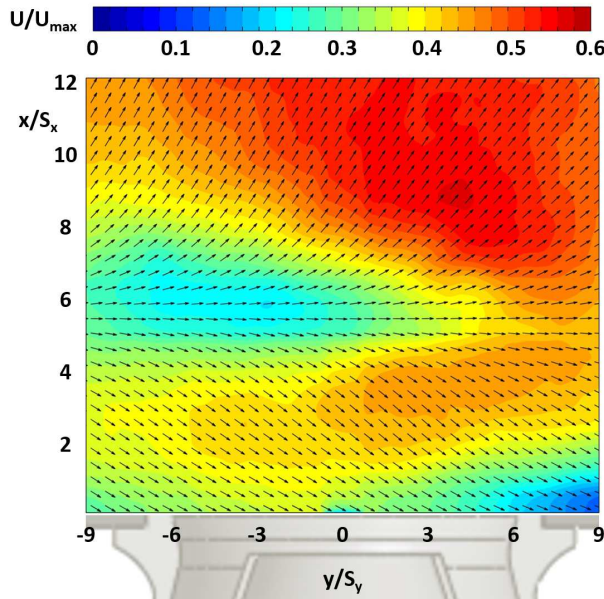


Figure 8: Flow field with no coolant injection on wall plane. Length of vectors are not proportional to velocity magnitude

314 of greater interest near the heat shield and liner corner. As expected minor discrepancies are observed in the
 315 the main recirculation region.

316 As already shown in [28], two well-distinct counter rotating vortices are generated by the 30° geometry
 317 with only the effusion system activated, while enabling the slot injection a coherent flow structure with high
 318 and positive velocity components in the axial direction is established. In this condition, the slot system seems
 319 to have a positive effect on film covering development inhibiting reverse flow near the liner.

320 Observing the corner regions in the 90° configuration with effusion coolant injection, a clockwise vortex
 321 can still be recognized as in the no cooling case. Nevertheless the high momentum of effusion jets in the
 322 positive z direction pushes the vortex center more downstream and closer to liner. A disturbing effect of this
 323 strong flow interaction is expected in terms of film cooling effectiveness in the early part of the liner. For
 324 $W = 3\%$ condition, slot coolant doesn't exhibits enough axial momentum to prevail on orthogonal effusion
 325 jets and is early lifted up, generating a low velocity region established near the heat shield underneath the
 326 swirling jet. However, similarly to 30° plate, slot injection tends to destroy the clockwise corner vortex,
 327 accomplishing only positive velocity components in the x direction near the wall.

328 As a general result, the 90° perforation tends to lift up the swirler jet, reducing its opening angle and

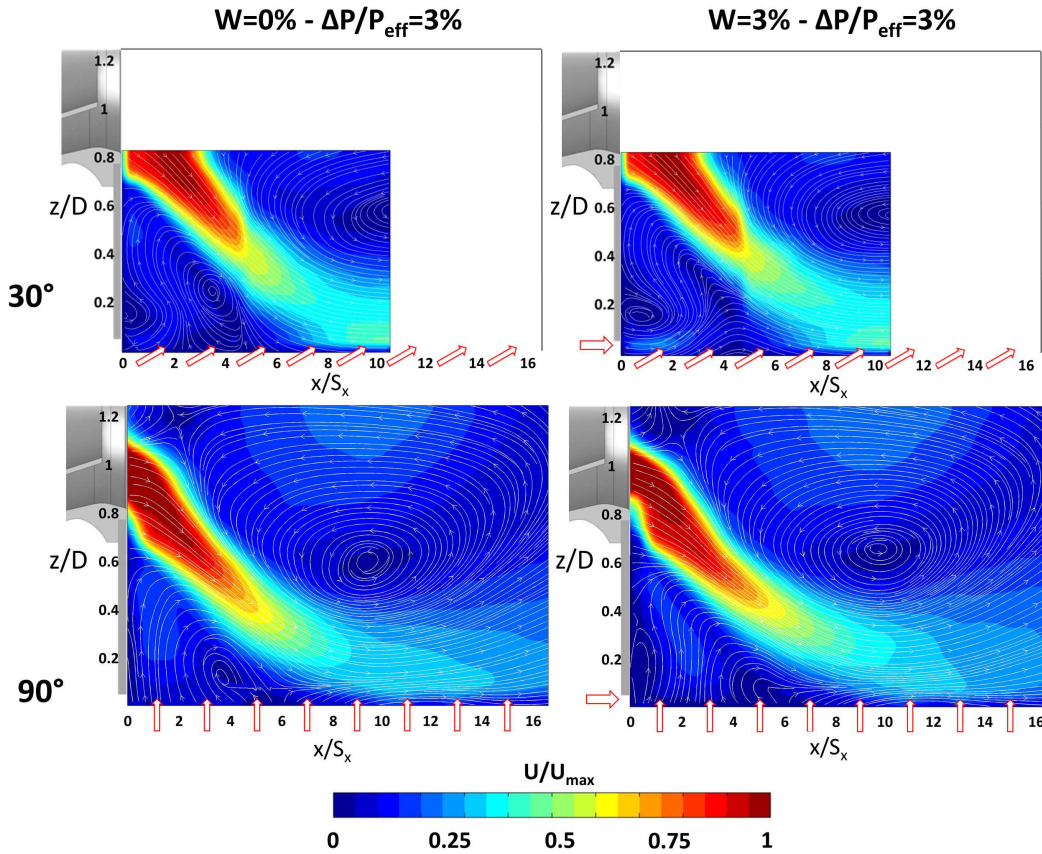


Figure 9: PIV results: flow field on measurements plane

329 moving slightly downstream the impingement region on the liner.

330

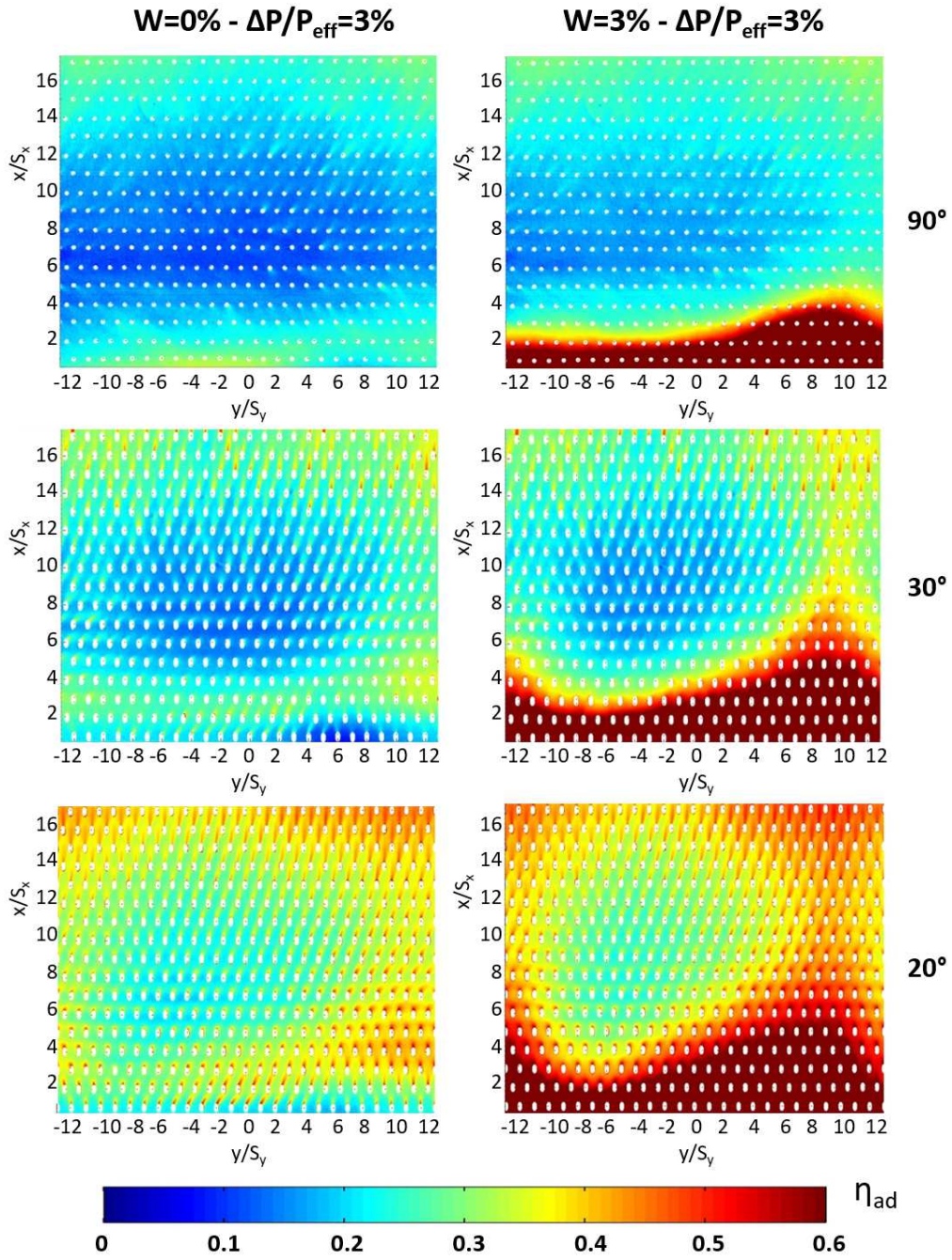


Figure 10: Adiabatic film cooling effectiveness distributions

331 *3.3. Adiabatic film cooling effectiveness measurements*

332 PSP campaign was aimed at investigating the adiabatic film cooling effectiveness distributions of three
 333 effusion plates under representative swirling flow, in order to explore the effect of injection angle on film
 334 covering. Tests were conducted imposing the swirlers pressure drop at the reference condition of $\Delta P/P =$
 335 3.5%. Effusion mass flow rates were set on the basis of multi-perforated plates pressure drop: three conditions
 336 were investigated corresponding to $\Delta P/P_{eff} = 1\%, 2\%, 3\%$. For each geometry, one test with slot cooling
 337 enabled was carried out in concurrence of the maximum level of effusion injection.

338 In Figure 10 are respectively reported from left to right the 2-D maps of η_{ad} obtained for 20°, 30° and 90°
 339 injection angle with a reference value of $\Delta P/P_{eff}$ equal to 3%. Distributions on the left column were obtained
 340 with the slot system disabled, while for the right column ones a coolant consumption equal to $W = 3\%$ was
 341 set. All maps are characterized by a non-symmetric central region with low effectiveness, corresponding to
 342 the stagnation region of the impinging jet highlighted by the PIV measurements. It is also worth to notice
 343 that probably part of the coolant is entrapped in the dome recirculation structures and is responsible of
 344 generating a streak with high effectiveness between about $y/S_y = 7$ and $y/S_y = 11$.

345 As expected, the highest film covering is achieved by the geometry with the lower inclination angle,

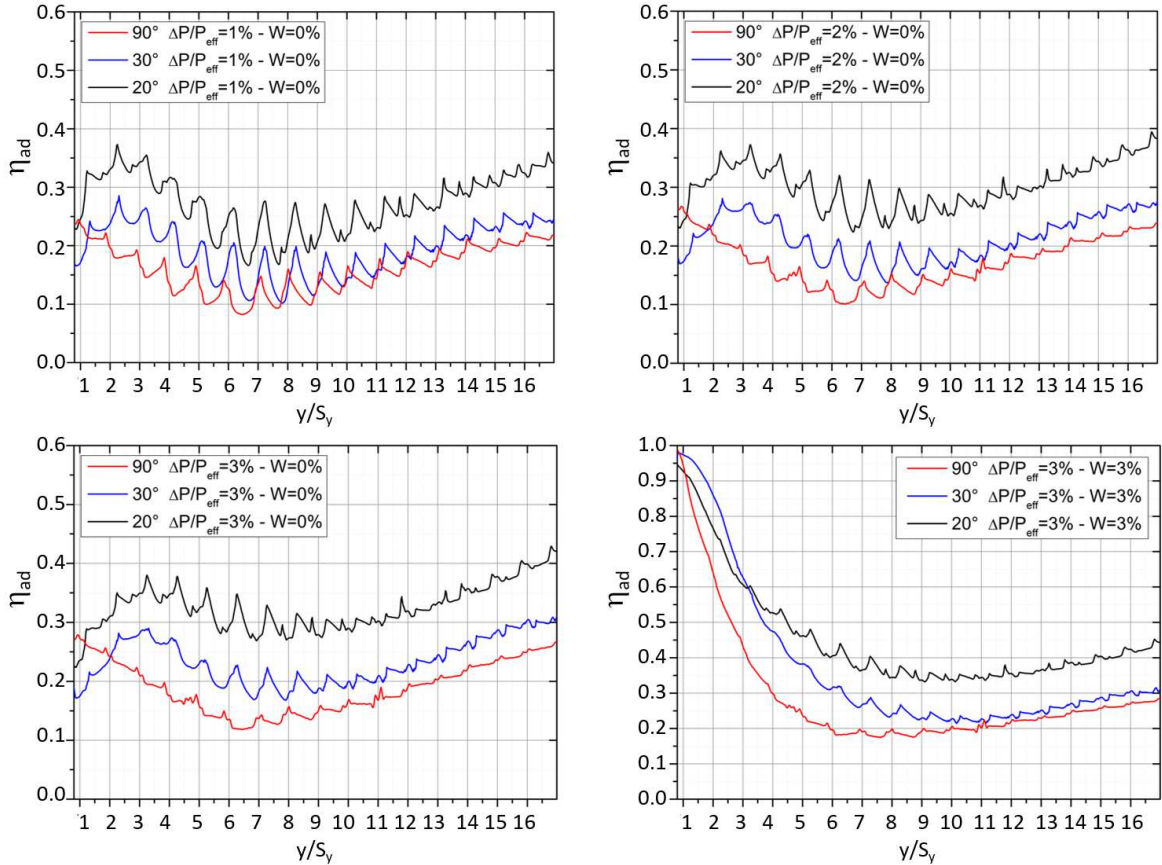


Figure 11: Laterally averaged adiabatic film cooling effectiveness profiles

346 where the coolant slant injection is capable to limit jet penetration and to take benefit from superposition
347 effects. The high resolution color maps obtained allow to appreciate the different shape of coolant wall traces
348 produced by each jet. Longer and more defined coolant imprints are observed for 20° geometry, while for 90°
349 coolant traces appears less coherent and more sensible to mainstream flow field.

350 The importance of using the slot system to start the film protection is clearly stated in the right column
351 distributions with an high film protection region obtained for $x/S_x < 2$. The role of slot cooling is appreciable
352 up to the jet stagnation region, while downstream approaching the exit, its effect is almost negligible.

353 For a more quantitative analysis, the laterally averaged distributions of adiabatic film cooling effectiveness
354 are reported in Figure 11. A comparison between the three multi-perforated plates is shown for all the three
355 levels of effusion mass flow rate, with the slot disabled, and for the reference condition with both the cooling
356 systems activated.

357 Apart from the expected increase of the film effectiveness in the final part of the liner ($x/S_x > 14$)
358 when cooling flow rate is increased (alongside with $\Delta P/P_{eff}$), similar evolution is observed for all the tested
359 conditions. Minimum adiabatic film cooling effectiveness values are clearly detected in the swirling jet
360 stagnation region ($x/S_x \approx 7$) due to the high turbulence levels generated by impingement phenomena that
361 tends to destroy the film and to lift up the effusion flow. Downstream ($x/S_x > 9 - 10$), superposition effect
362 leads to an almost linear growth of η_{ad} allowing to guarantee sufficient film protection also for the lower
363 effusion mass flow rates.

364 Results confirm the superiority of the 20° geometry in almost all the liner, with the gap versus the other
365 configurations that tends to increase enhancing the $\Delta P/P_{eff}$. With respect to 30° angle, a mean gain of
366 about 30% is achieved in terms of averaged film effectiveness with the 20° geometry. In the very first part of
367 the liner ($x/S_x < 2$) good results are also obtained by the 90° configuration due to the presence of reverse
368 flow near the wall, that leads to upstream film covering produced by the first rows of holes.

369 Distributions concerning the tests with slot coolant injected report approximately unitary values at the
370 liner entrance with the 30° plates showing the best results up to $x/S_x = 3$. Differences between the film
371 protection generated by the 30° and 90° inclination angle are appreciable in the first part of the liner
372 ($x/S_x < 9$), while downstream the values are almost comparable. The behaviour of the 90° test case with
373 slot injection in the early part of the liner is a consequence of the observed premature film lift up due to
374 strong flow recirculation (see 9): adiabatic film effectiveness values for normal holes plate are roughly half of
375 the values registered for the 20° case at rows 3-4.

376 A more comprehensive understanding of the obtained results can be achieved by the observation of the
377 Blowing Ratio distribution along the effusion cooling rows. A direct measure of the velocity at the outlet
378 of each effusion cooling hole was not possible and therefore BR is obtained assuming an uniform mass flow
379 rate across the perforation. This assumption is justified by the presence of a feeding plenum upstream of
380 the effusion plate and to small pressure variations on the mainstream side. The variation of BR along the
381 plate is therefore related mainly to the distribution of mainstream velocity close to liner wall. According

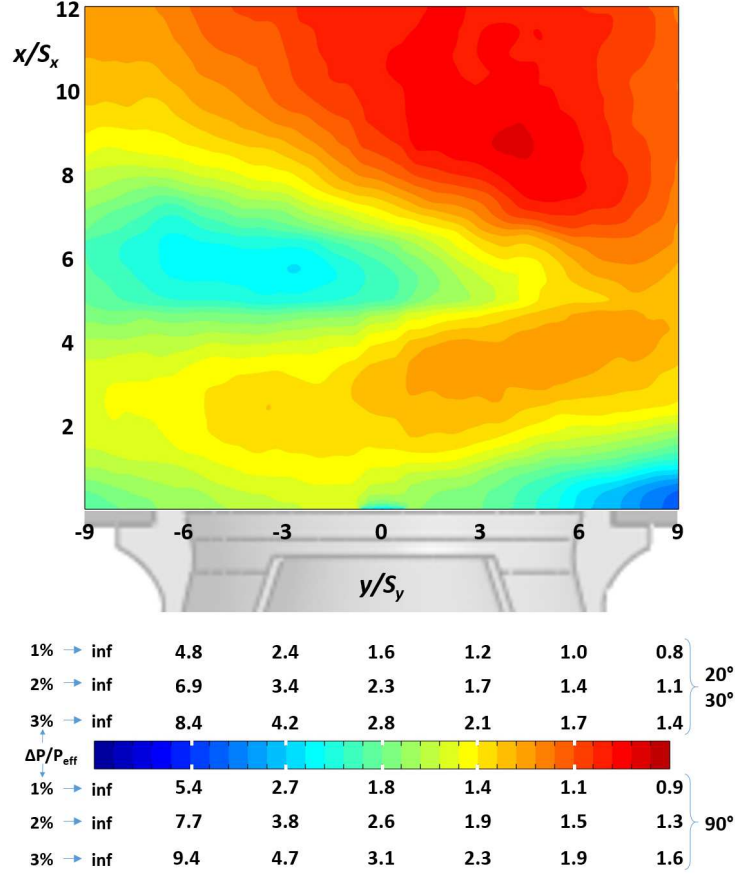


Figure 12: Distribution of the reference Blowing Ratio throughout the liner for the different cases investigated

382 to the mainstream velocity map obtained by PIV measurement on the Wall plane obtained with no coolant
 383 injection (Figure 8), it is possible to draw a distribution of a reference BR throughout the plate. Wall plane
 384 was considered as the reference location for mainstream velocity because it is located just at the outer edge
 385 of the slot (whose height is $5mm$): this plane also represents the nearest location to liner surface where the
 386 effect of effusion cooling jets is no longer observed. Reference BR is computed as follows:

$$BR = \frac{\dot{m}_{eff}}{\rho V_{main} A_{eff}} \quad (6)$$

387 where \dot{m}_{eff} is the effusion cooling mass flow, A_{eff} is the geometric cross section of the effusion perforation
 388 while ρV_{main} is obtained assuming a constant density in the mainstream and taking the velocity from the
 389 PIV wall plane measurements. Figure 12 shows the distribution of the above defined BR, with different
 390 scales for each level of pressure drop across the effusion plates (which implies different \dot{m}_{eff}) distinguishing
 391 between 90° and 20° - 30° according to the different discharge coefficients. It can be observed that, at the
 392 nominal level of effusion pressure drop (3%), the reference BR is always above 1.5 for all the cases, with values
 393 between 4-5 observed in the low mainstream velocity region of swirling jet impingement. The assumption of
 394 full penetration state for the film cooling regime is therefore definitely confirmed.

395 Focusing the attention on the initial part of the liner, the three maps of Figure 13 allow to deepen the
 396 impact of the slot system varying the effusion angle. The top figure shows the adiabatic film cooling effective-
 397 ness distribution obtained with only the slot system activated with the holes of the effusion plates plugged
 398 on the rear side to avoid air ingestion. Map is relative to the 90° geometry but an analogous behaviour
 399 was comprehensibly achieved also for the other configurations. A significant non-symmetric distribution in
 400 tangential direction is observed due to the macro flow structure which affects the test section and tends to
 401 direct towards the right side the flow near the liner surface [27], resulting in an high film protection region
 402 up to the third row of holes between $y/S_y \approx 5$ and $y/S_y \approx 10$. In the remaining parts of the map, high
 403 adiabatic film cooling effectiveness values are limited to the first row of holes.

404 The two following maps of Figure 13 were respectively obtained with 90° and 20° geometries and were
 405 carried out with both the slot and effusion system set at their reference conditions. Nevertheless, in this
 406 case the multi-perforated plates were fed with air, instead of Nitrogen, in order to take into account the
 407 fluid dynamic effect of coolant injection through the liner perforation without contributing to film protection
 408 detection (no free-oxygen tracer). Both the two distributions highlight a significant positive effect produced
 409 by effusion flow on the contribution of the slot coolant to the global film protection. In particular, the slant

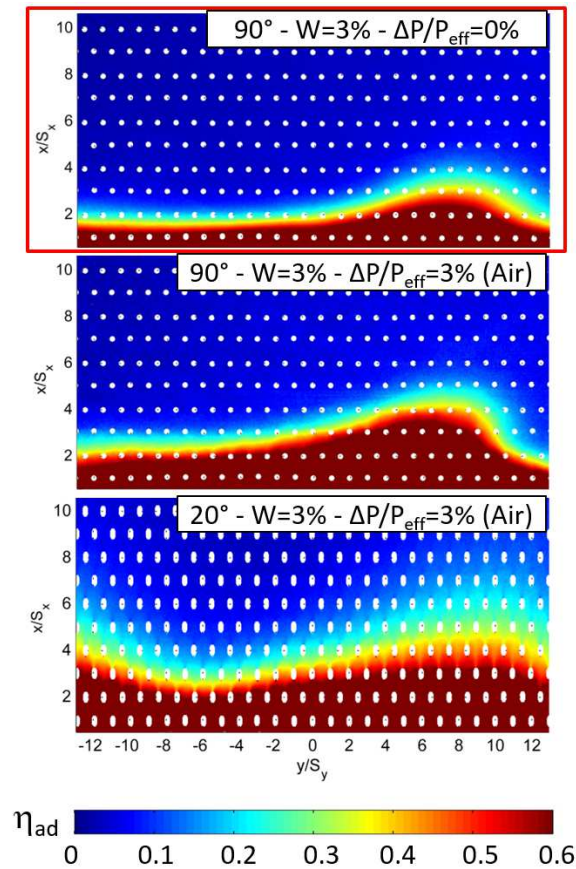


Figure 13: Adiabatic effectiveness distributions: slot injection

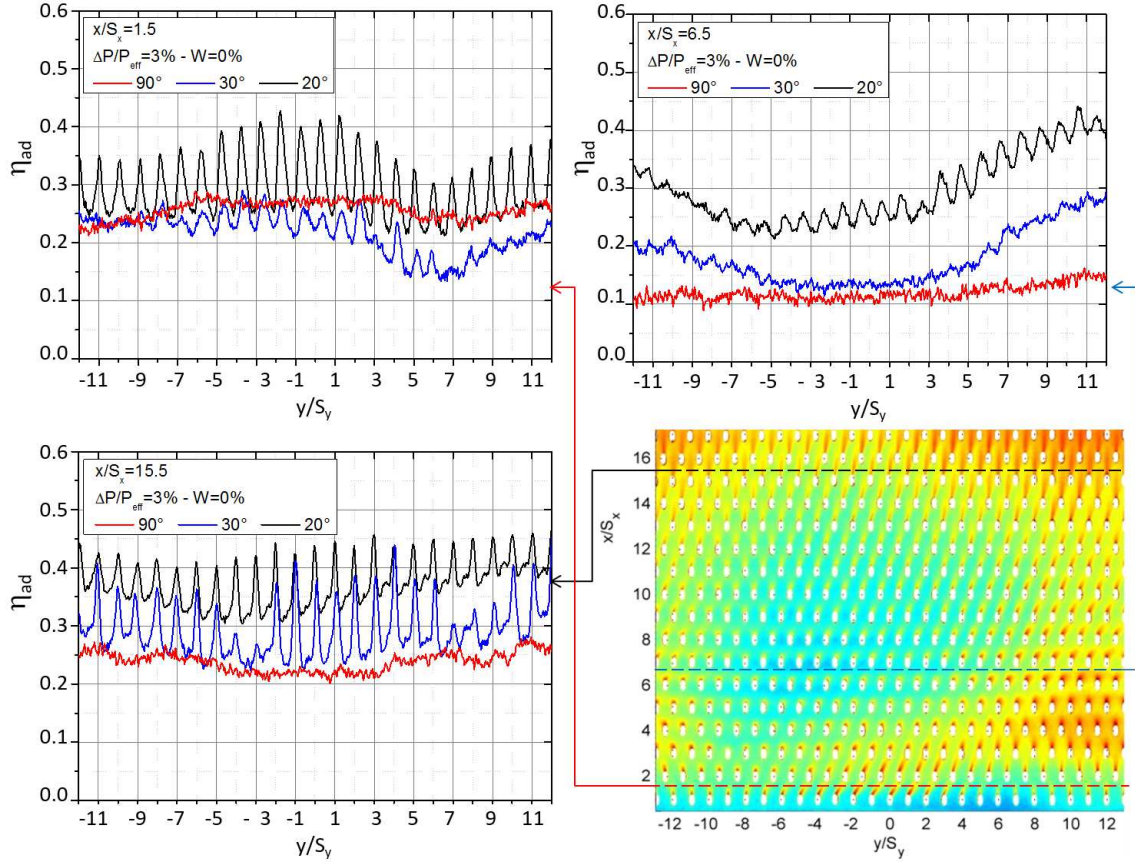


Figure 14: Lateral profiles of adiabatic effectiveness extracted at different axial positions

410 injection of the 20° liner produces inclined jets with high momentum that tend to energize the coolant flow
 411 structure exiting from the slot and to drag downstream its effect. Moreover, the distribution seems to be less
 412 affected by the test section flow field with a more constant behaviour alongside the y direction and with a
 413 film protection destroyed more gradually respect to the plate with perpendicular holes.

414 To better understand the behaviour of effusion film, three lateral profiles of adiabatic effectiveness have
 415 been extracted and reported in Figure 14: plots highlight the effect of the coolant injection angle at the more
 416 representative axial positions $x/S_x = 1.5; 6.5; 15.5$, respectively in the corner region, in the impingement zone
 417 and in the last part of the plate with more uniform flow structures. In the corner vortex region, the 90° plate
 418 shows film effectiveness values higher respect to the 30° especially in the $3 < y/S_y < 9$ zone where the slant
 419 angle performance seems strongly affected by the dome vortex structures. The superiority of the 20° plate is
 420 clearly represented in the impingement region where, despite the strong interactions with the main flow, the
 421 jets still present well defined coolant traces downstream of the injection points, especially for $y/S_y > 0$. It is
 422 interesting to observe that the 90° plate is not able to produce the high effectiveness streak at $y/S_y > 6$ and
 423 the η_{ad} is almost constant around the value 0.1. Finally, at $x/S_x = 15.5$ where the main flow field is more
 424 uniform the slant injection plates show their potentiality with pronounced and extended film traces.

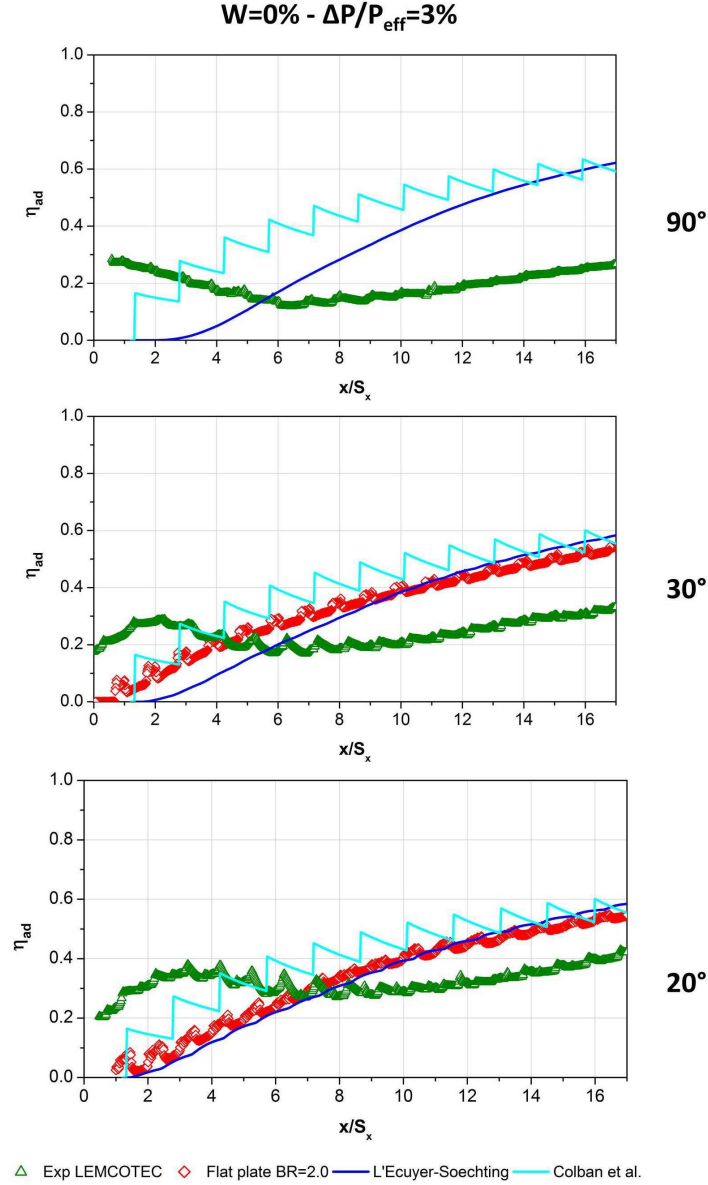


Figure 15: Comparisons of adiabatic film effectiveness measured in the present experimental campaign with literature correlations and experimental results obtained with a uniform mainstream velocity (only 20° and 30° cases)

425

426 3.4. Comparison with literature correlations

427 In order to assess how common literature correlations for adiabatic film effectiveness could be a reliable
 428 tool for the prediction of the investigated configurations, a comparison with formulas proposed by L'Ecuyer
 429 and Soechting [41] and by Colban et al. [43] was carried out. Both correlations are valid for a single row of
 430 holes on flat plate: the evaluation of the film effectiveness over the entire multi-perforated liner is realized
 431 by assuming a superposition of the contributions predicted for each row, recalling the superposition criteria

432 proposed by Sellers [44]. The correlation proposed by L'Ecuyer and Soechting is based on a large database
433 of experimental results for standard cylindrical holes with inclination angles between 30° and 90° . The
434 correlation proposed by Colban and coworkers was developed to predict adiabatic film effectiveness with
435 common fan shaped holes, but it can be used also for not shaped cylindrical perforations: in this case no
436 explicit dependency on the inclination angle is accounted in the expression.

437 Correlations were applied by assuming a uniform distribution of the measured mass flow rate over the
438 perforations, while the velocity evolution along the axial direction on the mainstream side was obtained by
439 laterally averaging the module of velocity retrieved by PIV measurements on the Wall plane (see 5): the
440 resulting blowing ratios for the effusion cooling rows in each case are exactly equivalent to values reported in
441 12. Results for the three investigated cases at $\Delta P/P_{eff} = 3\%$ without slot cooling injection are shown in 15.

442 As additional term of comparison, for inclined holes only (20° and 30°), 15 shows the measured adiabatic
443 film effectiveness obtained on the same hardware and with the same measurement technique but removing
444 the swirlers and therefore prescribing a uniform velocity in the mainstream. In these cases a constant blowing
445 ratio is obtained and the considered value (2.0) represents an averaged of the values observed for inclined
446 cases in the three sector rig. It is interesting to point out the quite good agreement between correlations
447 and experiments with uniform mainstream, confirming the reliability of the used correlations and of the
448 assumption of full superposition in presence of simple mainstream flow. On the contrary, when a realistic
449 swirling flow is considered, correlations are not able to properly catch the adiabatic film evolution in the early
450 part of liner affected by mainstream flow recirculation (upstream rows 6-7). Downstream the stagnation region
451 of the swirling jet, when the combustor mainstream starts to assume a more uniform behaviour, the adiabatic
452 film begins to point out a row by row superposition with a rate similar to what predicted by correlations
453 and to what observed in the simple flat plate configurations, as confirmed by an equivalent slope of adiabatic
454 film effectiveness curves along the x direction. This observation suggests a possible fruitful use of simple
455 correlations at least in the final part of the multiperforated liner.

456 4. Conclusions

457 An experimental study was presented dealing with the impact of holes injection angle on the performance
458 of an effusion cooling system. Test were conducted under realistic flow field conditions in a non-reactive three
459 sector planar rig equipped with a lean burn swirler injectors and a complete cooling scheme composed of a
460 slot for starter film cooling and a multi-perforated liner. The work was focused on the adiabatic film cooling
461 effectiveness measurement for three effusion plates with different injection angle (20° , 30° , 90°) under several
462 cooling conditions. A PSP technique was exploited to obtain detailed η_{ad} distributions and a supplementary
463 PIV survey was carried out to support the analysis.

464 Velocity maps show an apparently critical behaviour for the 90° injection angle where the orthogonal
465 coolant injection seems to be subjected to an high penetration in the mainstream, generating streamlines
466 oriented mainly in the z direction and leading to a premature lifting of the slot coolant. On the other hand

467 a slant injection from the effusion system helps the development of a more coherent slot coolant stream and
468 avoids the generation of reverse flow near the liner wall.

469 Adiabatic film cooling effectiveness maps show a deep impact of the injection angle on the effusion system
470 performance. As expected, the more tilted geometry (20°) leads to the best film protection, revealing a better
471 opposition to the coolant layer destruction caused by the impinging swirl jet and showing an advantageous
472 exploitation of superposition effects thanks to the limited penetration of the cooling jets. Furthermore the
473 slanted injection of effusion coolant has a beneficial impact on the slot system, extending more downstream
474 its effects.

475 In conclusion, the experimental survey allowed to deeply characterize a typical effusion system and to
476 investigated the impact of coolant injection angle on adiabatic film cooling effectiveness distribution. The
477 interaction with a typical combustion chamber flow field and the coexistence with other cooling method, as
478 the slot starter film cooling, were also analysed, providing fundamental information for the design of modern
479 combustor cooling scheme.

480

481 **Acknowledgement**

482 The authors wish to gratefully acknowledge LEMCOTEC (Low Emissions Core-Engine Technologies)
483 Consortium for the kind permission of publishing the results herein. LEMCOTEC is a Collaborative Project
484 co-funded by the European Commission within the Seventh Framework Programme (2007-2013) under the
485 Grant Agreement n 283216.

486 **References**

- 487 [1] S. M. Correa, Power generation and aeropropulsion gas turbines: From combustion science to combustion
488 technology, Symposium (International) on Combustion 27 (2) (1998) 1793–1807.
- 489 [2] H.-J. Bauer, New low emission strategies and combustor designs for civil aeroengine applications,
490 Progress in Computational Fluid Dynamics, An International Journal 4 (3-5) (2004) 130–142.
- 491 [3] R. Krewinkel, A review of gas turbine effusion cooling studies, International Journal of Heat and Mass
492 Transfer 66 (2013) 706 – 722.
- 493 [4] M. Martiny, A. Schulz, S. Wittig, Mathematical model describing the coupled heat transfer in effusion
494 cooled combustor walls, ASME Conference Proceedings (97-GT-329).
- 495 [5] M. Gerendás, K. Hoeschler, S. Th., Development and Modeling of Angled Effusion Cooling for the
496 BR715 Low Emission Staged Combustor Core Demonstrator, RTO AVT Symposium on "Advanced
497 Flow Management: Part B - Heat Transfer and Cooling in Propulsion and Power Systems" .

- 498 [6] A. Andreini, R. Becchi, B. Facchini, L. Mazzei, A. Picchi, A. Peschiulli, Effusion cooling system opti-
499 mization for modern lean burn combustor, ASME Conference Proceedings (GT2016-57721).
- 500 [7] N. Kasagi, M. Hirata, M. Kumada, Studies of full-coverage film cooling - 1. cooling effectiveness of
501 thermally conductive wall, American Society of Mechanical Engineers (Paper) (81 -GT-37).
- 502 [8] G. E. Andrews, A. A. Asere, M. L. Gupta, M. C. Mkpadi, Effusion cooling: the influence of number of
503 hole, Journal of Power and Energy **204**.
- 504 [9] G. E. Andrews, A. A. Asere, M. L. Gupta, M. C. Mkpadi, A. Tirmahi, Full Coverage Discrete Hole
505 Film Cooling: The Influence of the Number of Holes and Pressure Loss, ASME Conference Proceedings
506 (90-GT-61).
- 507 [10] G. E. Andrews, I. M. Khalifa, A. A. Asere, F. Bazdidi-Tehrani, Full Coverage Effusion Film Cooling
508 With Inclined Holes, ASME Conference Proceedings (95-GT-274).
- 509 [11] M. Martiny, A. Schulz, S. Wittig, Full-coverage film cooling investigations: adiabatic wall temperatures
510 and flow visualization, ASME Conference Proceedings (95-WA/HT-4).
- 511 [12] K. M. B. Gustafsson, T. Johansson, An Experimental Study of Surface Temperature Distribution on
512 Effusion-Cooled Plates, J. Eng. Gas Turbines Power. **123** (2001) 308–316.
- 513 [13] M. K. Harrington, M. A. McWaters, D. G. Bogard, C. A. Lemmon, K. A. Thole, Full-Coverage Film
514 Cooling With Short Normal Injection Holes, J. Turbomach. 123 (2001) 798–805.
- 515 [14] A. Martin, S. J. Thorpe, Experiments on Combustor Effusion Cooling Under Conditions of Very High
516 Free-Stream Turbulence, ASME Conference Proceedings (GT2012-68863).
- 517 [15] J. J. Scrittore, K. A. Thole, S. Burd, Investigation of Velocity Profiles for Effusion Cooling of a Combustor
518 Liner, ASME Conference Proceedings (GT2006-90532).
- 519 [16] P. Ligrani, M. Goodro, M. Fox, H.-K. Moon, Full-Coverage Film Cooling: Film Effectiveness and Heat
520 Transfer Coefficients for Dense and Sparse Hole Arrays at Different Blowing Ratios, J. Turbomach.
521 134 (6) (2012) 061039.
- 522 [17] N. W. Foster, D. Lampard, The Flow and Film Cooling Effectiveness Following Injection through a Row
523 of Holes, Journal of Engineering for Power 102 (3) (1980) 584.
- 524 [18] C. A. Hale, M. W. Plesniak, S. Ramadhyani, Film Cooling Effectiveness for Short Film Cooling Holes
525 Fed by a Narrow Plenum, J. Turbomach. 122 (3) (2000) 553.
- 526 [19] S. Baldauf, A. Schulz, S. Wittig, High-Resolution Measurements of Local Effectiveness From Discrete
527 Hole Film Cooling, J. Turbomach. 123 (4) (2001) 758.

- 528 [20] C. Yuen, R. Martinez-Botas, Film cooling characteristics of rows of round holes at various streamwise
529 angles in a crossflow: Part I. Effectiveness, *International Journal of Heat and Mass Transfer* 48 (23-24)
530 (2005) 4995–5016.
- 531 [21] T. Behrendt, C. Hassa, M. Gerendás, Characterization of Advanced Combustor Cooling Concept Under
532 Realistic Operating Conditions, *ASME Conference Proceedings* (GT2008-51191).
- 533 [22] A. Andreini, B. Facchini, A. Picchi, L. Tarchi, F. Turrini, Experimental and theoretical investigation
534 of thermal effectiveness in multiperforated plates for combustor liner effusion cooling, *J. Turbomach.*
535 136 (9).
- 536 [23] J. J. Scrittore, K. A. Thole, S. Burd, Experimental Characterization of Film-Cooling Effectiveness
537 Near Combustor Dilution Holes, *ASME Conference Proceedings* (GT2005-68704).
- 538 [24] A. Ceccherini, B. Facchini, L. Tarchi, L. Toni, D. Coutandin, Combined Effect of Slot Injection, Effusion
539 Array and Dilution Hole on the Cooling Performance of a Real Combustor Liner, *ASME Conference*
540 *Proceedings* (GT2009-48845).
- 541 [25] B. Wurm, A. Schulz, H. J. Bauer, M. Gerendás, Impact of Swirl Flow on the Cooling Performance of an
542 Effusion Cooled Combustor Liner, *J. Eng. Gas Turbines Power.* 134 (12) (2012) 121503–121503.
- 543 [26] B. Wurm, A. Schulz, H. J. Bauer, M. Gerendás, Cooling Efficiency for Assessing the Cooling Performance
544 of an Effusion Cooled Combustor Liner, *ASME Conference Proceedings* (GT2013-94304).
- 545 [27] A. Andreini, G. Caciolli, B. Facchini, A. Picchi, F. Turrini, Experimental Investigation of the Flow Field
546 and the Heat Transfer on a Scaled Cooled Combustor Liner With Realistic Swirling Flow Generated by
547 a Lean-Burn Injection System, *J. Turbomach.* 137 (3) (2014) 031012–031012, ISSN 0889-504X.
- 548 [28] A. Andreini, R. Becchi, B. Facchini, L. Mazzei, A. Picchi, F. Turrini, Adiabatic Effectiveness and Flow
549 Field Measurements in a Realistic Effusion Cooled Lean Burn Combustor, *J. Eng. Gas Turbines Power.*
550 138 (3) (2015) 031506–031506, ISSN 0742-4795.
- 551 [29] B. Ge, Y. Ji, Z. Chi, S. Zang, Effusion cooling characteristics of a model combustor liner at non-
552 reacting/reacting flow conditions, *Applied Thermal Engineering* 113 (2017) 902 – 911, ISSN 1359-4311.
- 553 [30] LEMCOTEC Low Emissions Core-Engine Technologies, <http://http://www.lemcotec.eu/>, 2011-
554 2016.
- 555 [31] S. Marinov, M. Kern, K. Merkle, N. Zarzalis, A. Peschiulli, F. Turrini, On Swirl Stabilized Flame
556 Characteristics Near The Weak Extinction Limit, *ASME Conference Proceedings* (GT2010-22335).
- 557 [32] D. Lilley, Swirl Flows in Combustion: a Review, *AIAA J.* 15 (8).

- 558 [33] Y. Fu, J. Cai, S.-M. Jeng, H. Mongia, Confinement effects on the swirling flow of a counter-rotating
559 swirl cup, ASME Conference Proceedings (GT2005-68622).
- 560 [34] G. E. Andrews, N. Ahmed, R. Phylaktou, P. King, Weak extinction in low NO_x gas turbine combustion,
561 ASME Conference Proceedings (2009) GT2009-59830.
- 562 [35] R. L. Simpson, R. L. Field, A Note on the Turbulent Schmidt and Lewis Numbers in a Boundary Layer,
563 International Journal of Heat and Mass Transfer 15 (1972) 177–180,.
- 564 [36] T. V. Jones, Theory for the use of foreign gas in simulating film cooling, International Journal of Heat
565 and Fluid Flow 20 (1999) 349–354.
- 566 [37] G. Caciolli, B. Facchini, A. Picchi, L. Tarchi, Comparison between PSP and TLC steady state techniques
567 for adiabatic effectiveness measurement on a multiperforated plate, Experimental Thermal and Fluid
568 Science 48 (0) (2013) 122–133.
- 569 [38] S. J. Kline, F. A. McClintock, Describing Uncertainties in Single Sample Experiments, Mechanical
570 Engineering 75 (1953) 3–8.
- 571 [39] J. Westerweel, Fundamentals of digital particle image velocimetry, Measurement Science and Technology
572 8 (12) (1997) 1379–1392.
- 573 [40] M. Gritsch, A. Schulz, S. Wittig, Effect of Crossflows on the Discharge Coefficient of Film Cooling Holes
574 With Varying Angles of Inclination and Orientation, J. Turbomach. 123 (4) (2001) 781–787.
- 575 [41] M. R. L’Ecuyer, F. O. Soechting, A model for correlating flat plate film cooling effectiveness forrows of
576 round holes, in: AGARD Heat Transfer and Cooling in Gas Turbines 12p (SEE N86-29823 21-07), 1985.
- 577 [42] L. Mazzei, A. Andreini, B. Facchini, F. Turrini, Impact of Swirl Flow on Combustor Liner Heat Transfer
578 and Cooling: A Numerical Investigation With Hybrid Reynolds-Averaged Navier–Stokes Large Eddy
579 Simulation Models, J. Eng. Gas Turbines Power. 138 (5) (2016) 051504.
- 580 [43] W. F. Colban, K. A. Thole, D. Bogard, A film-cooling correlation for shaped holes on a flat-plate surface,
581 Journal of Turbomachinery 133 (1) (2011) 011002.
- 582 [44] J. P. Sellers, Gaseous Film Cooling with Multiple Injection Stations, AIAA Journal 1 (9) (1963) 2154–
583 2156.